Langmuir

Article

pubs.acs.org/Langmuir

Photoelectrocatalytic Oxidation of Glutathione Based on Porous TiO_2–Pt Nanowhiskers

Guihua Chen,[†] Jianling Wang,[†] Changyu Wu,[†] Chen-zhong Li,[‡] Hui Jiang,[†] and Xuemei Wang*[,†]

[†]State Key Lab of Bioelectronics, Southeast University, Nanjing 210096, China

[‡]Nanobioengineering/Bioelectronics Lab, Department of Biomedical Engineering, Florida International University, 10555 West Flagler Street, Miami, Florida 33174, United States

ABSTRACT: The performance of TiO_2 nanoparticles is extremely attractive in various areas of chemical and biochemical engineering as they can effectively work by combining the photocatalytic property with various superior properties of the related nanostructure. The relevant photoelectrochemical detection has attracted considerable interest and shown potential applications in a wide range of areas. In this study, we have prepared new nanowhiskers of platinum-doped titanium dioxide (TiO_2–Pt), which could be further used to fabricate a novel nanointerface for the sensitive detection of biomolecules including glutathione (GSH). Our observations demonstrate that the sensitive TiO_2–Pt nanowhiskers biointerface could be readily fabricated by casting the TiO_2–Pt nanowhiskers suspension on a glassy carbon electrode (GCE), which could readily combine the photocatalytic and eletrocatalytic properties of TiO_2 nanocomposites to introduce a novel photoelectrocatalytic biosensor for GSH detection in real samples. Compared to other analysis strategies, the TiO_2–Pt nanowhiskers-modified GCE showed a considerably high sensitivity for the detection of GSH due to the excellent photoelectrocatalytic ability of the porous TiO_2–Pt nanowhiskers. Scanning electron microscopy (SEM), Raman spectroscopy, and electrochemical impedance spectroscopy have shown that Pt can readily blend with porous TiO_2 nanowhiskers and facilitate the relevant catalysis property of TiO_2, resulting in the enhanced photoelectrocatalytic effect. Thus, through the new strategy of the utilization of the excellent photoelectrocatalytic property of TiO_2–Pt nanocomposites, it is possible to realize the rapid electrochemical detection of glutathione with high sensitivity, low cost, and good reproducibility.

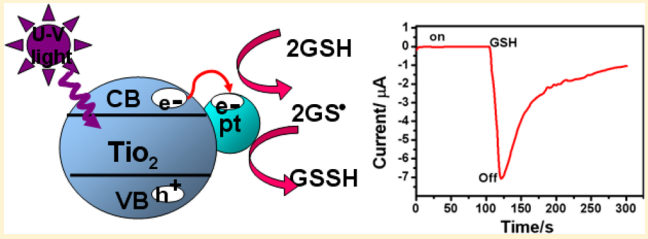

1. INTRODUCTION

Recently, TiO_2 has attracted more and more attention for its promising application in photocatalysts, sensors, biomedicine, et al.[1,2] The unique physical characteristics of nanostructured TiO_2, including crystallization, grain size, morphology, specific surface state and surface area, and porosity obviously influence the photocatalytic activity of TiO_2.[3−5] Over the last two decades, TiO_2 has been synthesized into various shapes, including nanoparticles, nanoporous materials, nanowires, nanorods, nanotubes, with functional groups which could be transformed under UV illumination. It is already known that, after UV illumination, the excited electrons (e^-) would be localized at the conduction band (CB) and the oxidative holes (h^+) would be localized at the valence band (VB), and these electron–hole pairs are strong oxidants which can be used as a photocatalytic agent. The excited electrons have been used to reduce selenium(VI) and mercury(II) for further atomic spectrometry while the oxidative holes have been shown to be readily scavenged by electron donors.[6−8] On the other hand, electron–hole pairs can be easily recombined, and thus, many strategies have been developed in order to enhance TiO_2 photocatalysis. It is already known that noble metals such as silver, gold, and platinum can enhance the reducibility of CB e^- due to the enrichment effect of CB e^- on the metal surface, and thus, they reduce the possibility of e^-–h^+ recombination.[9] Particularly, the TiO_2–Pt type is most attractive because it is a classic example of catalysts in which the catalytic property of the metal component is strongly modified by interaction with the active oxide support. Meanwhile, there are many porous structures on the surface of nano-TiO_2 whiskers where the important properties of the TiO_2 whiskers such as mesoporosity and the textual porosity could enlarge the surface–volume ratio, providing high specific area, and these nanoporous sites could readily provide doping positions for nano-Pt. Therefore, Pt-doped TiO_2 (TiO_2–Pt) nanocomposites retain not only the catalytic activity of metal nanoparticles (NPs) but also the intrinsic photocatalytic capacity of TiO_2. Moreover, TiO_2–Pt NPs could generate a Schottky barrier at the interface between Pt and TiO_2, which would effectively capture the photogenerated electrons, reduce the rate of electron–hole recombination, and improve quantum efficiency for photoelectrochemical systems. Thus, the nanocomposites of TiO_2–Pt whiskers (TiO_2–Pt nanowhiskers) could show an excellent photocatalytic property.

Received: June 11, 2012
Revised: July 23, 2012
Published: August 2, 2012

Glutathione is a tripeptide composed of glutamyl (Glu), cysteine (Cys), and glycine (Gly) and is a widely distributed biological substrate in living cells from microbes to higher organisms. In nature, glutathione exists in the oxidized (GSSG) and reduced (GSH) forms,[10,11] and the reduced form (GSH) is mainly found playing a direct or indirect role in gene expression regulation, enzyme activity and metabolic regulation, cell protection, amino acid transport, immune regulation, etc. Its viability in the reduced form may be a key factor in health maintenance. It has been well established that a decrease in GSH concentration may be correlated with aging and pathogenesis of several diseases, including rheumatoid arthritis, muscular dystrophy, amyotrophic lateral sclerosis, acquired immunodeficiency syndrome (AIDS), Alzheimer's disease, and Werner syndrome.[12−15] It is also already known that the level of glutathione in blood would reflect glutathione's status in less accessible tissues. Thus, biosensing of GSH in blood is essential for whole-body glutathione status and can be considered as an indicator of disease risk in humans.[16] The concentration of GSH in the cells varies from 0.0005 to 10 mmol L^{-1} under normal conditions.[11,17] In blood, more than 99% of GSH is found in the red blood cells (erythrocytes) where 16% of them are bound with proteins. Only 0.5% of GSH is found in the plasma.[18] Detection of glutathione by photometry,[18] electrochemical sensors, chromatography,[19,20] and immunoluminescence[21] has been reported; however, these detection strategies still need complicated pretreatments and have relatively low sensitivity. Therefore, it is necessary to find new approaches for glutathione biosensing.

Photoelectrochemical measurement is a newly developed technology for detecting biomolecules. Recently, Ju and coworkers[22] used free-base-porphyrin-functionalized zinc oxide nanoparticles for photoelectrochemical oxidation of cysteine. By coupling photocatalytic agents with electrocatalytic detection, photoelectrochemical biosensors may integrate the advantages of both optical and electrochemical sensors.[23] Thus, this technique has attracted considerable interest and shows potential applications in a wide range of areas. In this contribution, we have explored the possibility of the utilization of the porous TiO_2−Pt nanocomposites to develop a unique photoelectrochemical nanointerface for highly sensitive detection of glutathione. In addition, we used acetyl ferrocene as an electrochemical mediator since ferrocene and its derivatives are the most widely used ones with good stability in both oxidized and reduced forms, rapid response to many electroactive substances, independent pH, inertness with oxygen, regeneration at low potential, and fast electron transfer.[24] Our results demonstrate that the TiO_2−Pt nanowhiskers-modified electrode could be utilized as a promising biointerface for detection of glutathione with high sensitivity, fast speed, low cost, low toxicity and good reproducibility.

2. EXPERIMENTAL SECTION

2.1. Reagents and Solution. Reduced glutathione (GSH) was purchased from Sunshine Biotechnology (SunShineBio, China). *N*,*N*-Dimethylformamide (DMF), 5-sulfosalicylic acid, $EDTANa_2$ and acetyl ferrocene were also acquired from SunShine Biotechnology. Platinum-doped titanium dioxide (TiO_2−Pt) nanowhiskers were kindly provided by Prof. Xiaohua Lu from Nanjing University of Technology and prepared as previously reported.[25] All other chemicals were of analytical grade and were used as received.

Disodium hydrogen phosphate and sodium dihydrogen phosphate were used to prepare phosphate buffer (PBS), and the pH value was adjusted accordingly. A stock solution of 1.0×10^{-2} mol L^{-1} GSH was prepared daily by dissolving 3.07 g GSH in PBS (pH 7.1), and then diluting with PBS for other GSH concentrations. The solution was kept in a refrigerator at 4 °C in the dark. A solution of 0.1 mol L^{-1} acetyl ferrocene was prepared in DMF. All other solutions were prepared by using deoxygenated doubly distilled water.

2.2. Apparatus and Procedures. Scanning electron microscopy (SEM) was performed by using a Hitachi S-4800 scanning electron microscope (Hitachi, Tokyo, Japan). Resonance Raman spectra were recorded on a microscopic confocal Raman microscope (Jobin Yvon HR800 confocal Raman system) from 200 cm^{-1} to 800 cm^{-1}, using a 533 nm diode laser excitation on an 1800-line. The ultrapure water (Ω18.2 M > cm^{-1}) was prepared from Milli-Q purification system (Millipore Co. Ltd. U.S.A.). Electrochemical measurements were performed on a CHI660B electrochemical workstation at room temperature under the nitrogen flow environment. A three-electrode system was used in the electrochemical study, which contains the TiO_2−Pt nanowhiskers film-modified glassy carbon electrode (GCE) as the working electrode, a Pt electrode as the counterelectrode, and a saturated calomel electrode (SCE) as the reference electrode. The electrochemical impedance spectrum (EIS) measurements were carried out on an Autolab PGSTAT302N system (Eco Chemie, Netherlands) by using the above three-electrode system. All solutions were purged with high-purified nitrogen for at least 10 min prior to each set of experiments. The nitrogen environment was then maintained over the solutions in the electrochemical cell during the respective measurements.

2.3. Procedures for Preparation and Modification of GC Electrode. Initially, the GCE (Φ = 3 mm) was polished with rough and fine sandpapers. Then its surface was polished to mirror smoothness with the 0.05 μm alumina slurry. Eventually, the GCE was thoroughly washed by ultrasonic treatment in doubly distilled water for 3 min before the modification. Meanwhile, in order to prepare the TiO_2−Pt nanowhiskers films on GCE, the TiO_2−Pt nanowhiskers (1 mg/mL) were added into 1 mL double-distilled water, and the resultant mixture was ultrasonicated for about 20 min. Afterward, the suspension of TiO_2−Pt nanowhiskers (8 μL) was dropped on the surface of the GCE and was dried naturally in air. Then the modified electrodes could be irradiated at a distance of 10 cm by UV light at different time points.

2.4. Procedures for Preparation and Modification of ITO Electrode. The ITO electrodes were cleaned with NaOH (1 mol L^{-1}) and H_2O_2 (30%), and then washed with acetone, alcohol, and double-distilled water by ultrasonication. After drying at room temperature, 10 μL of the TiO_2−Pt rodlike nanowhiskers suspension was coated onto the ITO electrode and dried at room temperature to obtain a TiO_2−Pt nanowhiskers-modified ITO electrode. During the experiments, the UV light was used to study the photocatalysis on GSH. In this procedure, an electrochemical droplet was induced with TiO_2−Pt nanowhiskers-modified ITO electrode as working electrode, silver wire as the reference electrode, and platinum wire as the counter electrode. All experiments were conducted in PBS buffer (0.1 mol L^{-1}, pH 7.1).

2.5. Procedures for Real Sample Preparation. The blood samples were treated according to the literature.[19] In detail, 10 mL of blood samples were freshly taken from the hospital in tubes containing heparin. Then samples were centrifuged 1000 × *g* for 15 min at 4 °C, and the plasma was discarded. The erythrocytes were washed three times with phosphate buffer solution, and aliquots of the erythrocytes were hemolyzed (1:1 v/v) in 1 mmol L^{-1} $EDTANa_2$ solution. After preparing the hemolysis, 10% (w/v) 5-sulfosalicylic acid was added, followed by vigorous shaking and centrifugation at 1000 × *g* for 10 min at 4 °C. The supernatant was collected for the GSH determination.

3. RESULTS AND DISCUSSION

3.1. SEM and Raman Spectroscopy Characterization of TiO_2−Pt Nanowhiskers. The morphologies and the mesoporous structures of TiO_2−Pt nanowhiskers were characterized by SEM. Figure 1A shows the SEM image of porous TiO_2−Pt nanowhiskers, indicating that the morpholo-

dx.doi.org/10.1021/la302355b | *Langmuir* 2012, 28, 12393−12399

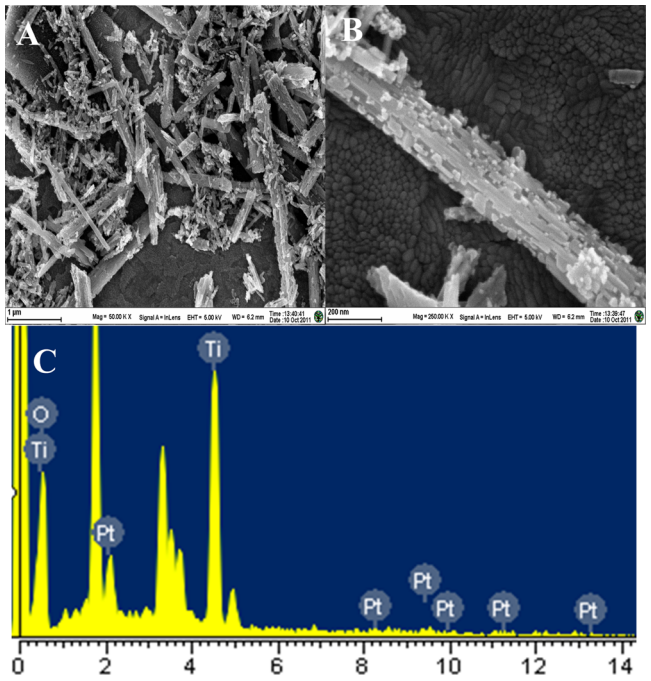

Figure 1. SEM images of TiO_2–Pt-modified ITO electrode: (A) the morphologies and the microsurface structures of TiO_2–Pt nanowhiskers. (B) a single TiO_2–Pt nanowhisker. (C) The EDS pattern of the modified electrode.

gies and the microsurface structures of TiO_2–Pt nanowhiskers are rodlike, with a diameter of 50–150 nm and a length of 500–1000 nm, which are advantageous for the construction of a robust homogeneous film for the formation of a biosensor. It is noted that there are many mesopores which can provide binding sites for Pt nanoparticles (NPS). Figure 1B is the typical characterization of a single nanowhisker. We can see clearly that Pt nanoparticles locate on the TiO_2 rodlike nanowhisker. With Pt nanoparticles, the catalyst activity increased greatly due to the production of a Schottky barrier on the surface of the TiO_2, where the photoelectrons could readily move to metal when illuminated by UV light and be captured by metal while the hole can be freely spread to the TiO_2 semiconductor surface.[20]

Meanwhile, Raman spectroscopic study of TiO_2–Pt nanowhiskers has been further explored. Figure 2A shows the Raman spectroscopy of TiO_2–Pt nanowhiskers with the typical peaks at 144, 399, 518, 640 cm^{-1} (curve b), which are the same as those for the Lu group,[25] whereas the characteristics of the pure TiO_2 nanowhiskers (curve a) appears at 146, 395, 512, 638 cm^{-1}, as also reported in the literature.[21,23] It is noted from Figure 2B that, apart from the first peak, the Raman intensity of the three characteristic bands of TiO_2–Pt nanowhiskers are 7540, 7020, 10312, while the ones of TiO_2 are 5903, 5636, 8809. This shows that the Raman intensities of the three characteristic bands of TiO_2–Pt nanowhiskers increase apparently when compared with that of the nano TiO_2, with strengths enhanced by 27.7%, 24.6%, 17.1%, respectively. This phenomenon can be attributed to the electron-transfer effect of TiO_2–Pt whiskers related to the surface-state energy levels of the TiO_2 semiconductor.[26] This is of great importance for photocurrent generation in photovoltaic applications, where the anatase phase of TiO_2 has a larger surface area and faster electron transport than the rutile phase.[27] Moreover, after Pt was doped on the surface of TiO_2 nanowhiskers, the TiO_2 anatase nanocrystalline structure retained the three characteristics bands, indicating that the functionalization of TiO_2 nanowhiskers with Pt did not damage the conjugation of the nano TiO_2.[28] It could be observed from EDS (Figure 1C) that Ti, O, and Pt are the main elements and the content of Pt is about 0.5%.

3.2. EIS Characterization of the Nanointerface of TiO_2–Pt Whiskers. EIS is a method of measuring the impedance value of the electrode surface during the process of frequency variation that is able to offer various properties of the interface of the electrode and solution, including the electrode impedance, the capacity of the electric double layer, and the surface charge-transfer resistance (R_{ct}).[29] In the Nyquist diagrams, the semicircle diameter of EIS is equal to R_{ct}. For the TiO_2 photocatalytic reaction, a decrease in the radius of resistance means a charge transfer more likely occurred, which is beneficial to relevant catalytic activity. Overall, the semicircle diameter of EIS corresponds to the size of the charge-transfer resistance and photoelectron–holes separation efficiency. The efficiency of charge and hole separation is faster with UV light irradiation.[30] Figure 2C illustrates the Nyquist diagrams of TiO_2 nanowhiskers (curve,

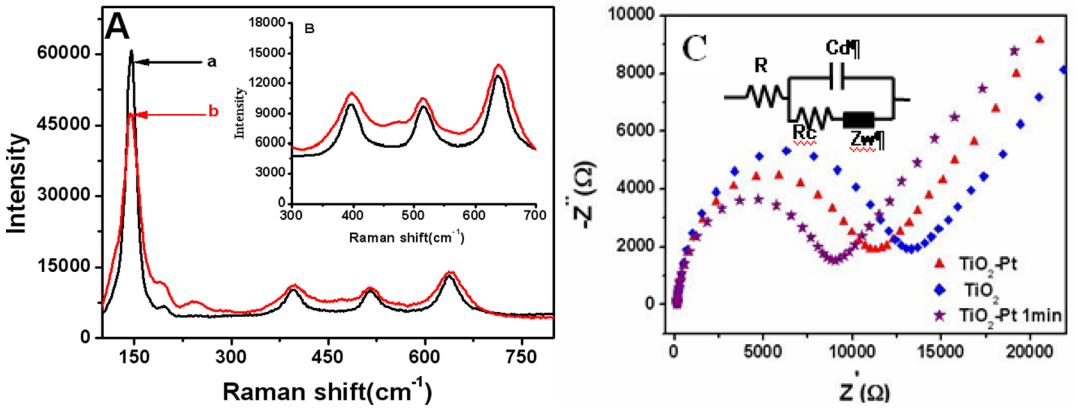

Figure 2. (A) Raman spectrum of Pt-doped anatase TiO_2 nanowhiskers (b) and pure anatase TiO_2 nanowhiskers (a). (B) Amplified Raman spectrum from 300 to 700 cm^{-1}. (C) Nyquist plots for the Faradaic impedance measurements of a 1.0 mM of 1:1 $K_3[Fe(CN)_6]/K_4[Fe(CN)_6]$ performed on TiO_2–Pt-modified electrode with 1 min UV illumination (curve ★), TiO_2–Pt-modified electrode without UV illumination (curve, ▲ [red]) and TiO_2-modified electrode (curve, ◆ [blue]).

dx.doi.org/10.1021/la302355b | *Langmuir* 2012, 28, 12393–12399

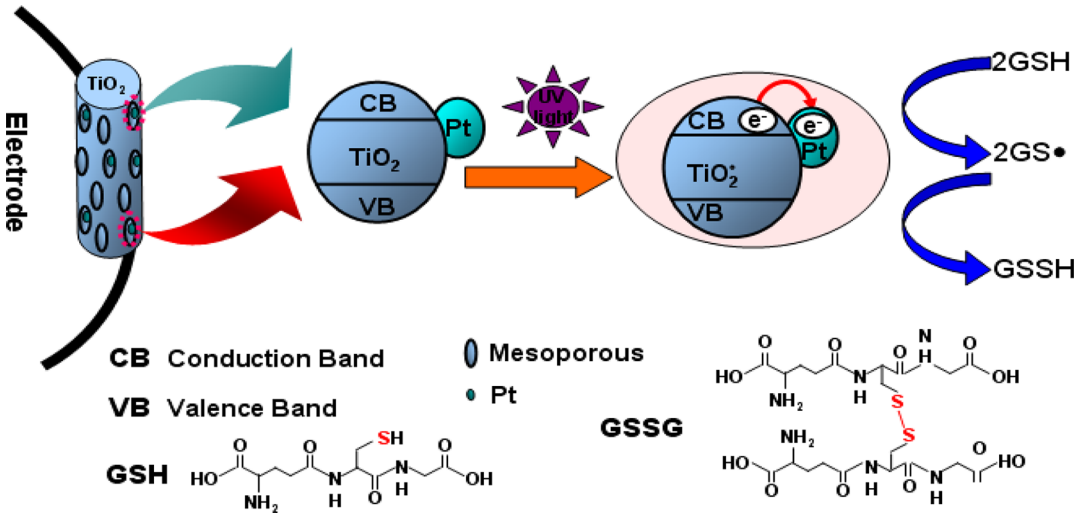

Figure 3. Schematic illustration of photoelectrocatalytic oxidation of GSH based on TiO_2–Pt/GCE.

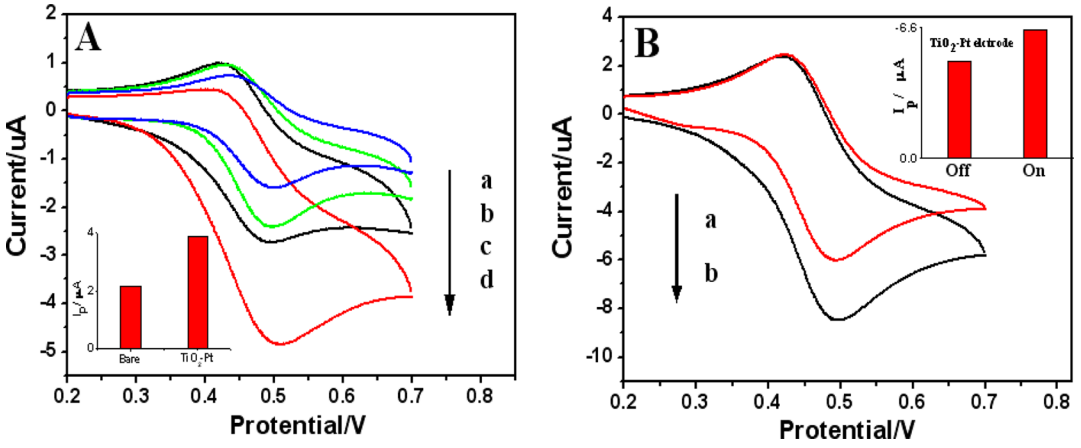

Figure 4. (A) Cyclic voltammograms of bare GCE (a, b) and TiO_2–Pt nanowhiskers/GCE(c, d) in the absence (a, c) and presence (b, d) of 50 μmol L^{-1} GSH in 0.1 mol L^{-1} PBS (pH 7.1) containing 0.1 mmol L^{-1} acetyl ferrocene. Inset A: changes of I_p between bare GCE and TiO_2–Pt nanowhiskers-modified GCE in presence of GSH. (B) Cyclic voltammograms of TiO_2–Pt nanowhiskers/GCE in the presence of 50 μmol L^{-1} GSH: (a) No illumination, (b) after 1 min illumination in 0.1 mol L^{-1} PBS (pH 7.1) containing 0.1 mmol L^{-1} acetyl ferrocene. Inset B: changes of I_p between no illumination and after 1 min illumination in presence of 50 μmol L^{-1} GSH.

◆ [blue]) and TiO_2–Pt nanowhiskers-modified electrode without UV light (curve, ▲ [red]) and under UV light (curve ★) in the presence of electrochemical probe i.e., 1.0 mol L^{-1} of 1:1 $K_3[Fe(CN)_6]/K_4[Fe(CN)_6]$ in PBS (pH 7.1). It can be seen that at the TiO_2 nanowhiskers-modified electrode, a semicircle with R_{et} of 1.3 kΩ was obtained. However, the R_{ct} of the TiO_2–Pt nanowhiskers electrode was reduced to 1.1 kΩ (curve, ▲ [red]), suggesting that a significant acceleration of the $[Fe(CN)_6]^{3-/4-}$ redox reaction occurred due to the presence of the Pt nanoparticles. Meanwhile, it was interesting to find that the R_{ct} of the TiO_2–Pt nanowhiskers-modified electrode under UV light irradiation was sharply reduced to 0.9 kΩ. From Figure 2C, we found that the R_{ct} of TiO_2–Pt nanowhiskers under the dark state was larger, suggesting that the TiO_2–Pt nanowhiskers under the dark state need to overcome a greater energy barrier, while the R_{ct} of TiO_2–Pt nanowhiskers decreased because TiO_2–Pt nanowhiskers remarkably reduced the activity of the electrode reaction barrier.[31]

3.3. Photoelectrocatalytic Oxidation of GSH on TiO_2–Pt Whiskers. As we all know, after UV illumination, the excited electrons (e^-) move to the conduction band (CB), and the oxidative holes (h^+) move to the valence band (VB), and these electron–hole (e^-–h^+) pairs are strong oxidants which can be used as a photocatalysis. Moreover, platinum can make the e^- transfer from CB to Pt nanoparticle, reducing the possibility of e^-–h^+ recombination.[9] In this way, there are more electron–hole pairs on the TiO_2–Pt nanowhiskers which can be utilized in photocatalysis. In view of this, we have used the UV light to illuminate the TiO_2–Pt nanowhiskers-modified GCE, as shown in Figure 3. The effective electrocatalytic activity of TiO_2–Pt/GCE could be readily detected by cyclic voltammetry. It is observed that TiO_2–Pt nanowhiskers-modified GCE can remarkably increase the anodic peak current of the relevant ferrocene. As shown in Figure 4, compared with that of the bare GCE, the peak current (I_p) of the TiO_2–Pt nanowhiskers-modified GCE was considerably enhanced. Meanwhile, the related anodic peak current in the presence of GSH is much larger than that in the absence of GSH (Figure 4A), and the anodic current has been efficiently enhanced for about 32% after the UV illumination (Figure 4B), indicating that the specific nanointerface of porous TiO_2–Pt nano-

dx.doi.org/10.1021/la302355b | Langmuir 2012, 28, 12393–12399

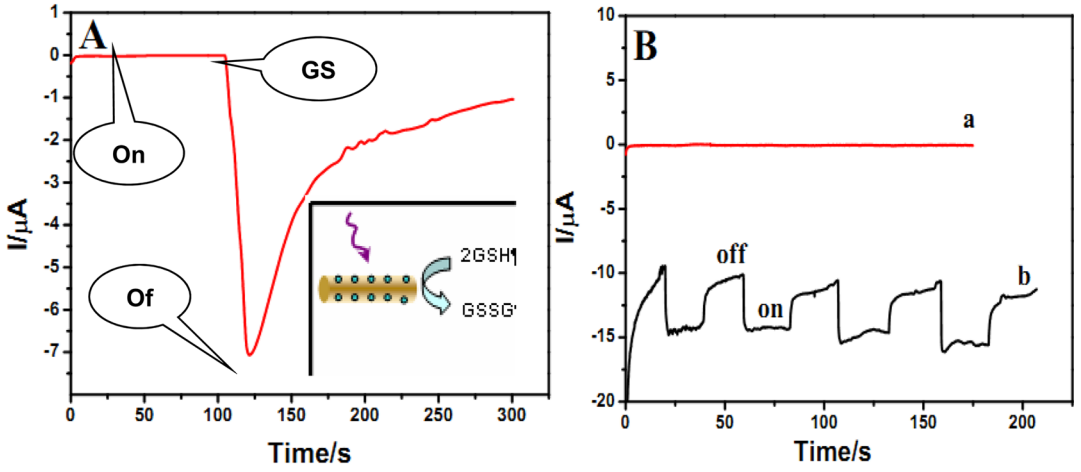

Figure 5. (A) $I-T$ curve of photocurrent responses of TiO_2–Pt nanowhiskers before adding 50 μmol L^{-1} GSH and after adding GSH with the light on and off. Inset A: schematic illustration of TiO_2–Pt nanowhiskers based on ITO electrode with the technology of droplet electrochemical experiment. (B) $I-T$ curve of the switch effects in the absence (a) and presence (b) of 50 μmol L^{-1} GSH with the electrolyte of 0.1 mol L^{-1} PBS (pH 7.1) containing 0.1 mmol L^{-1} acetyl ferrocene.

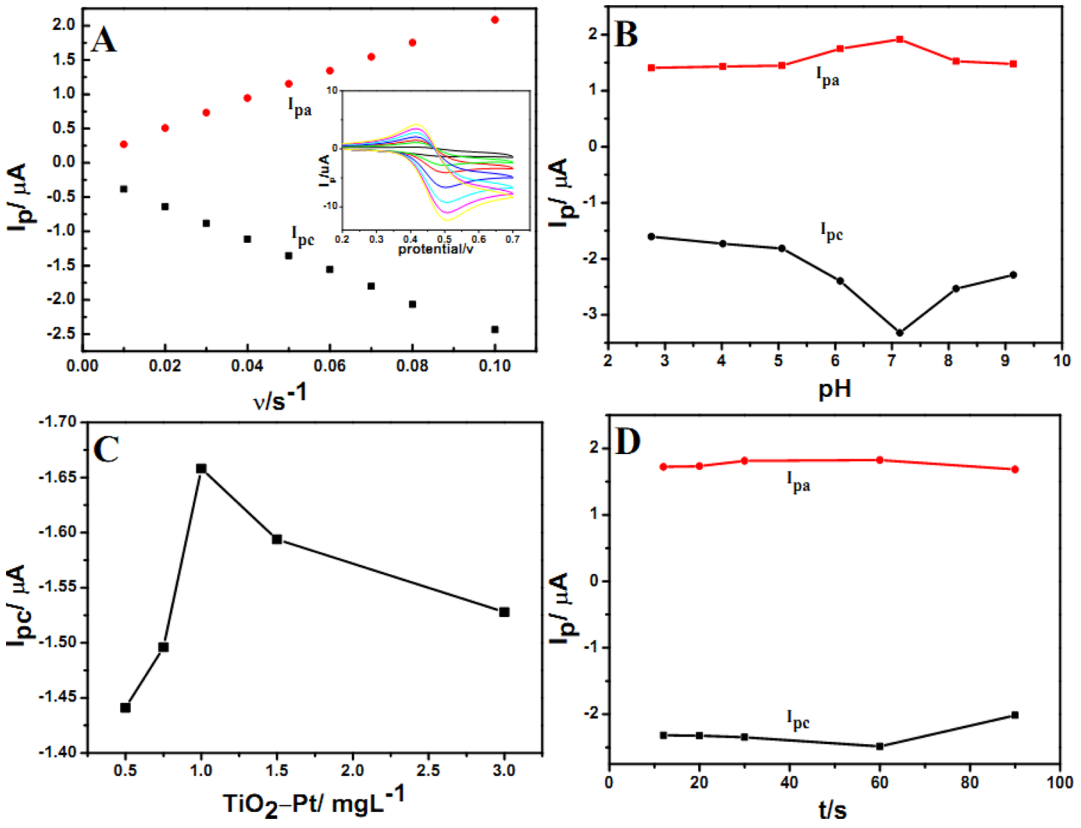

Figure 6. Optimization study on the experimental conditions for the electrocatalytic oxidation of GSH. (A) dependence of scan rate; (B) pH effect; (C) effect of TiO_2–Pt nanowhiskers concentrations; (D) effect of illumination time.

whiskers could significantly improve the electrocatalytic oxidation of GSH. This effective electrocatalytic oxidation could be attributed to many porous structures on the surface of TiO_2–Pt nanowhiskers where the important properties such as mesoporosity and the textual porosity could enlarge the surface–volume ratio, providing high specific area.

On the basis of these observations, we have further explored the relevant photoelectrocatalytic oxidation process of GSH based on TiO_2–Pt nanowhiskers/ITO. Before addition of GSH, the TiO_2–Pt nanowhiskers-modified ITO electrode showed a photocurrent of 17.6 nA in 0.1 mol L^{-1} PBS (pH 7.1), whereas the photocurrent on nano-TiO_2-modified ITO electrode is about 5.6 nA, indicating that the nano-Pt-doped TiO_2 whiskers could significantly enhance the relevant photoelectrocatalytic effect. Upon addition of 10 μL of 1 mmol L^{-1} GSH, the photocurrent is observed to increase up to 7.01 μA. When turning off the UV light, the photocurrent remarkably decreases, as shown in Figure 5A. The switch on–switch off experiment is shown in Figure 5B. Comparing Figure 2B (a) with (b), we found that the switch effect only happened

dx.doi.org/10.1021/la302355b | *Langmuir* 2012, 28, 12393–12399

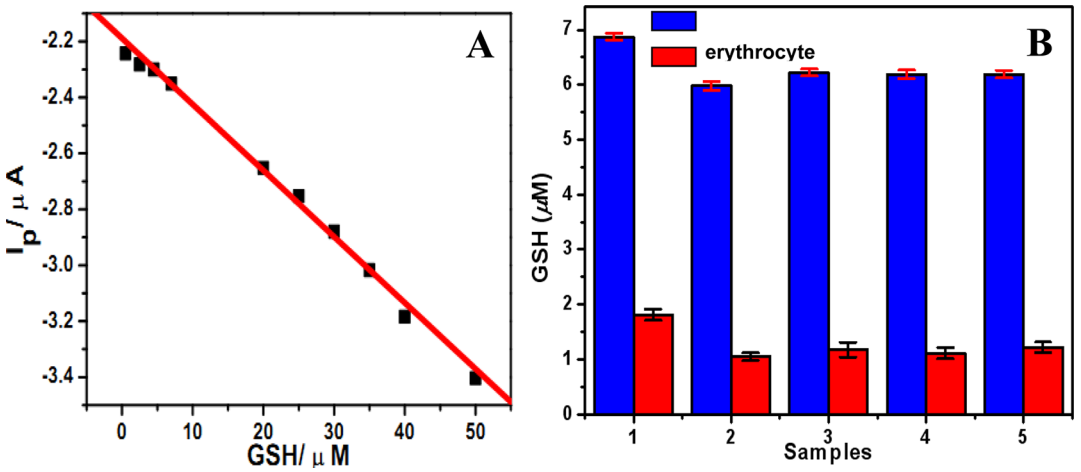

Figure 7. (A) Linear relationship of electrocatalytic oxidation current of GSH on TiO_2−Pt nanowhiskers with different concentrations of GSH. (B) Data obtained from determination of GSH in human erythrocyte and erythrocyte with 5 μmol L^{-1} GSH.

when containing GSH. This can also prove that the TiO_2−Pt nanocomposite is a photocatalyst during the procedures of GSH oxidation. It is obvious that, upon illuminating the surface of the TiO_2−Pt nanowhiskers, there are rich electron−hole pairs which are strong oxidants that can oxidize the GSH, resulting in the remarkable photocurrent.

3.4. Photoelectrocatalytic Determination of GSH in Real Samples. Initially, the effect of the potential scan rate (ν) on the electrocatalytic property of TiO_2−Pt nanowhiskers toward electrooxidation of GSH was studied by cyclic voltammetry. As shown in Figure 6A, the results demonstrate that the peak currents of the voltammograms are linearly proportional to ν with the linear correlation of 0.999 for both I_{pa} and I_{pc}, indicating that there is a surface-controlled electrochemical reaction.

It is well-known that the electrochemical behavior of GSH relies on the pH value of the solution, because the GSH is characterized by the number of dissociation constants: pK_{a1} = 2.12, pK_{a2} = 3.59, pK_{a3} = 8.75, pK_{a4} = 9.65.[1] Therefore, the electrochemical behavior of GSH on TiO_2−Pt nanowhiskers-modified electrode was studied by cyclic voltammetry in the range of different pH values (Figure 6B). Our observations indicate that, when using the TiO_2−Pt nanowhiskers-modified electrode, the anodic peak current of GSH could reach a maximum value at pH 7.1 and then decrease gradually with the increasing pH values. Therefore, the pH of 7.1 was selected as an optimal pH value for the determination of GSH.

As we all know, TiO_2 is a semiconductor that would affect electron transfer rate. Our observations illustrate that 1 mg/mL is the best modification amount of TiO_2 nanocomposites on the electrode (Figure 6C). Meanwhile, the relevant illumination time has little effect on the photocurrent in this study (Figure 6D), so we chose 1 min for UV illumination time.

On the basis of the above optimized studies, the photoelectrocatalytic detection of GSH in reality has been further explored in 0.1 mol L^{-1} PBS (pH 7.1) containing 0.1 mmol L^{-1} acetyl ferrocene at the surface of TiO_2−Pt nanowhiskers by using a CV study, which exhibits an anodic peak potential at 520 mV (GSH anodic peak potential) vs Ag|AgCl|KCl (3 mol L^{-1}) (Figure 7A). The results show the rapid response of the TiO_2−Pt nanowhiskers-modified electrode to GSH with the mediated oxidation peak current of GSH related to its concentration. The photoelectrocatalytic plot was linear in the concentration range of 0.5−40 μmol L^{-1} with the linear correlations of 0.994 (Figure 7A), with the detection limit of 0.1 μmol L^{-1}. The range of this linearity depends on the amount of mediator in the electrode matrix. This observation indicates that the linear response range was wider than those obtained by the electrogenerated chemiluminescence of quantum dots (0.024−0.214 mmol L^{-1})[32] and the photoelectrochemical detection (0.05−2.4 mmol L^{-1}),[23] while the detection limit of 0.1 μmol L^{-1} was lower than the limits of 8.3 μmol L^{-1}[32] and 0.03 mmol L^{-1}[23] by the previous method.

Since the concentration of GSH in the cells varies from 0.0005 to 10 mmol L^{-1} under normal conditions,[8,9] photoelectrocatalytic detection of glutathione based on the nanointerface of TiO_2−Pt nanowhiskers provides a new strategy for the sensitive and rapid detection of GSH in biological samples with a steady signal response. Evidently, the proposed TiO_2−Pt nanowhiskers-based photoelectrocatalytic oxidation shows promising applications in the rapid determination of GSH at point-of-care testing, making the possibility of immediate diagnosis and treatment a reality. As shown in Figure 7B, the TiO_2−Pt nanowhiskers-based biosensor has been utilized to detect five normal blood samples, where the relevant concentration of GSH was found to be 1.83, 1.05, 1.19, 1.13, and 1.24 μmol L^{-1} respectively. When spiking 5 μmol L^{-1} GSH standard solution to these blood samples, the relevant concentration of GSH detected in the blood was 6.9, 6, 6.24, 6.2, and 6.2 μmol L^{-1}, respectively. The recovery was 101.03, 99.17, 100.87, 101.14, and 99.2% respectively. It is evident that the TiO_2−Pt nanowhiskers-based biosensor could accurately and sensitively detect GSH in real samples of erythrocytes.

4. CONCLUSIONS

In summary, we have prepared the new nanointerface from TiO_2−Pt nanowhiskers, which have been further explored to fabricate a new biosensor to rapidly detect GSH with high sensitivity and low cost. The results demonstrate that the TiO_2−Pt nanowhiskers-modified GCE could readily combine the photocatalytic and eletrocatalytic properties of TiO_2 nanocomposites to introduce a novel photoelectrocatalytic biosensor for GSH detection in real samples. Compared to other analysis strategies, the nanointerface of TiO_2−Pt/GCE showed a considerably high sensitivity for the fast detection of GSH, which may play an important role for early diagnosis of

dx.doi.org/10.1021/la302355b | Langmuir 2012, 28, 12393−12399

some relevant diseases such as cancer, AIDS, diabetes, and atherosclerosis in clinical application.

AUTHOR INFORMATION

Corresponding Author

*E-mail: xuewang@seu.edu.cn.

Notes

The authors declare no competing financial interest.

ACKNOWLEDGMENTS

This research has been supported by the National Basic Research Program of China (2010CB732404), the National Natural Science Foundation of China (21175020), and the Doctoral Fund of Ministry of Education of China (20090092110028).

REFERENCES

(1) Bavykin, D. V.; Walsh, F. C. Elongated Titanate Nanostructures and Their Applications. *Eur. J. Inorg. Chem.* **2009**, *8*, 977−997.

(2) Sakai, N.; Wang, R.; Fujishima, A.; Watanabe, T.; Hashimoto, K. Effect of Ultrasonic Treatment on Highly Hydrophilic TiO_2 Surfaces. *Langmuir* **1998**, *14*, 5918−5920.

(3) Yu, J.; Wang, G.; Cheng, B.; Zhou, M. Effects of Hydrothermal Temperature and Time on the Photocatalytic Activity and Microstructures of Bimodal Mesoporous TiO_2 Powders. *Appl. Catal. B* **2007**, *69*, 171−180.

(4) Ohtani, B.; Ogawa, V.; Nishimoto, S. Photocatalytic Activity of Amorphous Anatase Mixture of Titanium(IV) Oxide Particles Suspended in Aqueous Solutions. *J. Phys. Chem. B* **1997**, *101*, 3746−3752.

(5) Subramanian, V.; Wolf, E. E; Kamat, P. V. Catalysis with TiO_2/Au Nanocomposites. Effect of Metal Particle Size on the Fermi Level Equilibration. *J. Am. Chem. Soc.* **2004**, *126*, 4943−4950.

(6) Wang, Q. Q.; Liang, J.; Qiu, J. H.; Huang, B. L. Online Prereduction of Selenium(VI) with a Newly designed UV/TiO_2 Photocatalysis Reduction Device. *J. Anal. At. Spectrom.* **2004**, *19*, 715−716.

(7) Liang, J.; Wang, Q. Q.; Huang, B. L. Electrochemical Vapor Generation of Selenium Species after Online Photolysis and Reduction by UV-Irradiation under Nano TiO_2 Photocatalysis and Its Application to Selenium Speciation by HPLC Coupled with Atomic Fluorescence Spectrometry. *Bioanal. Chem.* **2005**, *381*, 366−372.

(8) Yin, Y. M.; Liang, J.; Yang, L. M.; Wang, Q. Q. Vapor Generation at a UV/TiO_2 Photocatalysis Reaction for Determination and Speciation of Mercury by AFS and HPLC-AFS. *J. Anal. At. Spectrom.* **2007**, *22*, 330−334.

(9) Linsebigler, A. L.; Lu, G.; Yates, J. T. Photocatalysis on TiO_2 Surfaces: Principles, Mechanisms, and Selected Results. *Chem. Rev.* **1995**, *95*, 735−758.

(10) Meister, A.; Anderson, M. E. Glutathione. *Annu. Rev. Biochem.* **1983**, *52*, 711−760.

(11) Meister, A. Glutathione Metabolism and Its Selective Modification. *J. Biol. Chem.* **1988**, *263*, 17205−17208.

(12) Gambir, J. K.; Lali, P.; Jain, A. K. Correlation between Blood Antioxidant Levels and Lipid Peroxidation in Rheumatoid Arthritis. *Clin. Biochem.* **1997**, *30*, 351−355.

(13) Samiec, P. S.; Drews-Botsch, C.; Flagg, E. W.; Kurtz, J. C.; Sternberg, P., Jr.; Reed, R. L.; Jones, D. P. Glutathione in Human Plasma: Decline in Association with Aging, Age-Related Macular Degeneration, and Diabetes. *Free Radical Biol. Med.* **1998**, *24*, 699−704.

(14) Bonnefont-Rousselot, D.; Lacomblez, L; Jaudon, M. C.; Lepage, S.; Salachas, F.; Bensimon, G.; Bizard, C.; Doppler, V.; Delattre, J.; Meininger, V. Blood Oxidative Stress in Amyotrophic Lateral Sclerosis. *J. Neuro. Sci.* **2000**, *178*, 57−62.

(15) Cecchi, C.; Latorraca, S.; Sorbi, S.; Iantomasi, T.; Favilli, F.; Vincenzini, M. T.; Liguri, G. Gluthatione Level Is Altered in Lymphoblasts from Patients with Familial Alzheimer's Disease. *Neurosci. Lett.* **1999**, *275*, 152−154.

(16) Pastore, A.; Feredici, G.; Bertini, E.; Piemonte, F. Analysis of Glutathione: Implication in Redox and Detoxification. *Clin. Chim. Acta* **2003**, *333*, 19−39.

(17) Knapen, M. F. C. M.; Zusterzeel, P. L. M.; Peters, W. H. M.; Steegers, E. A. P. Glutathione and Glutathione-Related Enzymes in Reproduction. *Eur. J. Obstetr. Gynecol. Reprod. Biol.* **1999**, *82*, 171−184.

(18) Mills, B. J.; Lang, C. A. Differential Distribution of Free and Bound Glutathione and Cyst(e)ine in Human Blood. *Biochem. Pharmacol.* **1996**, *52*, 401−406.

(19) Griffith, O. W. Determination of Glutathione and Glutathione Disulfide Using Glutathione Reductase and 2-Vinylpyridine. *Anal. Biochem.* **1980**, *106*, 207−212.

(20) Sun, B.; Boolchand, P.; Smirniotis, P. G. Visible Light Photocatalysis with Platinized Rutile TiO_2 for Aqueous Organic Oxidation. *Langmuir* **2005**, *21*, 11397−11403.

(21) Chen, X. B.; Mao, S. S. Titanium Dioxide Nanomaterials: Synthesis, Properties, Modifications, and Applications. *Chem. Rev.* **2007**, *107*, 2891−2959.

(22) Tu, W. W.; Dong, Y. T.; Lei, J. P.; Ju, H. X. Photoelectrochemistry of Free-Base-Porphyrin-Functionalized Zinc Oxide Nanoparticles and Their Applications in Biosensing. *Chem.—Eur. J.* **2011**, *17*, 9440−9447.

(23) Tu, W. W.; Dong, Y. T.; Lei, J. P.; Ju, H. X. Low-Potential Photoelectrochemical Biosensing Using Porphyrin-Functionalized TiO_2 Nanoparticles. *Anal. Chem.* **2010**, *82*, 8711−8716.

(24) Raoof, J. B.; Ojani, R.; Beitollahi, H.; Hossienzadeh, R. Electrocatalytic Determination of Ascorbic Acid at the Surface of 2,7-bis (Ferrocenyl Ethyl) Fluoren-9-one Modified Carbon Paste Electrode. *Electroanalysis* **2006**, *18*, 1193−1201.

(25) Bai, Y; Li, W; Liu, C; Yanng, Z. H.; Feng, X.; Lu, X. H.; Chan, K. Stability of Pt Nanoparticles and Enhanced Photocatalytic Performance in Mesoporous Pt-(anatase/TiO_2(B)) Nanoarchitecture. *J. Mater. Chem.* **2009**, *19*, 7055−7061.

(26) Yang, L. B.; Jiang, X.; Ruan, W. D.; Zhao, B.; Xu, W. Q.; Lombardi, J. R. Direct Observation of Enhanced Raman Scattering for Molecules Adsorbed on TiO_2 Nanoparticles: Charge-transfer Contribution. *J. Phys. Chem. C* **2008**, *112*, 20095−20098.

(27) Park, N. G.; Lagemaat, J.; Frank, A. J. Comparison of Dye-Sensitized Rutile- and Anatase-Based TiO_2 Solar Cells. *J. Phys. Chem. B* **2000**, *104*, 8989−8994.

(28) Imahori, H.; Hayashi, S.; Umeyama, T.; Eu, S.; Oguro, A.; Kang, S.; Matano, Y.; Shishido, T.; Ngamsinlapasathian, S.; Yoshikawa, S. Comparison of Electrode Structures and Photovoltaic Properties of Porphyrin-Sensitized Solar Cells with TiO_2 and Nb, Ge, Zr-added TiO_2 Composite Electrodes. *Langmuir* **2006**, *22*, 11405−11411.

(29) Song, Z.; Li, Q.; Gao, L. Preparation and Properties of Nano-TiO_2 Powders. *J. Mater. Sci. Technol.* **1997**, *13*, 321−323.

(30) Hsu, C.; Lee, K.; Huang, J.; Lin, C; Lee, C.; Wang, L.; Tsai, S.; Ho, K. EIS Analysis on Low Temperature Fabrication of TiO_2 Porous Films for Dye-Sensitized Solar Cells. *Electrochim. Acta* **2008**, *53*, 7514−7522.

(31) Gomes, W. P.; Vanmaekelbergh, D. Impedance Spectroscopy at Semiconductor Electrodes: Review and Recent Developments. *Electrochim. Acta* **1996**, *41*, 967−973.

(32) Wang, Y.; Lu, J.; Tang, L. H.; Chang, H. X.; Li, J. H. Graphene Oxide-Amplified Electrogenerated Chemiluminescence of Quantum Dots and Its Selective Sensing. *Anal. Chem.* **2009**, *81*, 9710−9715.